Species-specific disruption of STING-dependent antiviral cellular defenses by the Zika virus NS2B3 protease

Qiang Ding[a], Jenna M. Gaska[a], Florian Douam[a], Lei Wei[a], David Kim[a], Metodi Balev[a], Brigitte Heller[a], and Alexander Ploss[a,1]

[a]Department of Molecular Biology, Lewis Thomas Laboratory, Princeton University, Princeton, NJ 08544

Edited by Michael B. A. Oldstone, The Scripps Research Institute, La Jolla, CA, and approved May 30, 2018 (received for review February 25, 2018)

The limited host tropism of numerous viruses causing disease in humans remains incompletely understood. One example is Zika virus (ZIKV), an RNA virus that has reemerged in recent years. Here, we demonstrate that ZIKV efficiently infects fibroblasts from humans, great apes, New and Old World monkeys, but not rodents. ZIKV infection in human—but not murine—cells impairs responses to agonists of the cGMP-AMP synthase/stimulator of IFN genes (cGAS/STING) signaling pathway, suggesting that viral mechanisms to evade antiviral defenses are less effective in rodent cells. Indeed, human, but not mouse, STING is subject to cleavage by proteases encoded by ZIKV, dengue virus, West Nile virus, and Japanese encephalitis virus, but not that of yellow fever virus. The protease cleavage site, located between positions 78/79 of human STING, is only partially conserved in nonhuman primates and rodents, rendering these orthologs resistant to degradation. Genetic disruption of STING increases the susceptibility of mouse—but not human—cells to ZIKV. Accordingly, expression of only mouse, not human, STING in murine STING knockout cells rescues the ZIKV suppression phenotype. STING-deficient mice, however, did not exhibit increased susceptibility, suggesting that other redundant antiviral pathways control ZIKV infection in vivo. Collectively, our data demonstrate that numerous RNA viruses evade cGAS/STING-dependent signaling and affirm the importance of this pathway in shaping the host range of ZIKV. Furthermore, our results explain—at least in part—the decreased permissivity of rodent cells to ZIKV, which could aid in the development of mice model with inheritable susceptibility to ZIKV and other flaviviruses.

flavivirus | Zika virus | antiviral immunity | viral evasion | species tropism

Infections with flaviviruses remain major contributors to morbidity and mortality in the human population (1). Approximately 390 million people contract dengue virus (DENV) annually, with roughly 96 million developing clinically symptomatic disease (2). Yellow fever virus (YFV) causes about 200,000 infections each year, of which 15–50% are fatal. As is the case for these two viruses, Zika virus (ZIKV) is also a small, enveloped, positive-sense (+), single-stranded RNA virus. Isolated incidents of ZIKV infection were first reported in the 1950s (3), but in recent years, ZIKV has caused massive outbreaks in French Polynesia (2013–2014) and South America (2015–2016) (4). Studies have suggested that an enhancement of NS1 antigenemia in infected hosts may have facilitated ZIKV transmission during recent epidemics by promoting the virus' infectivity and prevalence in mosquitoes (5).

ZIKV is an arthropod-borne virus that can also be transmitted through sexual contact and has thereby spread to millions of individuals over the last 2 y, predominantly in the Americas. Although acute infection is largely asymptomatic in immunocompetent patients, ZIKV is associated with a variety of neurological and neurodevelopmental disorders, including Guillain-Barré syndrome in adults and microcephaly in newborns, presumably by direct infection of neural progenitor cells in the fetal brain during pregnancy (6, 7). ZIKV can also cause male infertility via direct infection of testicular tissue (8). Over the last few years, remarkable progress has been made in developing strategies to prevent and treat ZIKV infection. Although there are still no licensed antivirals, numerous independently conducted, small molecular screens have yielded promising leads with great potency in cell culture and animal models (9–14). Similarly, a plethora of vaccination approaches have successfully induced protective immunity in preclinical models (15–19).

Despite these advances, the host tropism of ZIKV remains poorly understood. As observed for other members of the *Flaviviridae* family, including DENV, YFV, and West Nile virus (WNV), ZIKV presumably has other zoonotic reservoirs. Nonhuman primate (NHP) species are likely candidates given that ZIKV was originally isolated in 1947 from the serum of a sentinel rhesus macaque used for yellow fever surveillance (20). In efforts to model ZIKV infection, several species have been inoculated experimentally, including neonatal pigs, chicken embryos, rhesus and cynomolgus macaques, and rodents (reviewed in ref. 21). Immunocompetent mice, a species which evolutionarily diverged from humans about 65 Mya (22), are not susceptible to ZIKV infection. The basis for this apparent resistance is due—at least in part—to differences in how ZIKV is sensed by the innate immune system in rodents and the limited ability of ZIKV to evade antiviral defenses. Previous studies have demonstrated that mice with impaired type I IFN signaling succumb to ZIKV infection (8, 23–25). Collectively, these observations

Significance

To shed light on the host range of Zika virus (ZIKV), we surveyed the virus' ability to infect cells of evolutionarily diverse species. ZIKV replicates efficiently in human, great ape, Old and New World monkey, but not rodent cells. These observations correlated with ZIKV's ability to blunt the cGAS/STING signaling pathway in all primate cells tested but not in mice. We demonstrate that an enzyme shared by many flaviviruses (NS2B3) is responsible for functionally inactivating this antiviral defense. Our results highlight the importance of the cGAS/STING pathway in shaping the host range of ZIKV, which in turn may guide the development of murine models with inheritable susceptibility to ZIKV and other flaviviruses.

Author contributions: Q.D. and A.P. designed research; Q.D., J.M.G., F.D., L.W., D.K., M.B., B.H., and A.P. performed research; Q.D. and A.P. analyzed data; and Q.D. and A.P. wrote the paper.

The authors declare no conflict of interest.

This article is a PNAS Direct Submission.

[1]To whom correspondence should be addressed. Email: aploss@princeton.edu.

This article contains supporting information online at www.pnas.org/lookup/suppl/doi:10.1073/pnas.1803406115/-/DCSupplemental.

Published online June 18, 2018.

argue that the evasion of antiviral defenses by ZIKV is not conserved across species.

In this study, we aimed to systematically analyze the host tropism of ZIKV across a diverse panel of species, including human, bonobo, chimpanzee, gorilla, orangutan, rhesus and pig-tailed macaques, olive baboon, squirrel monkey, and mouse. We demonstrate that cells from all these species except mouse are readily susceptible to ZIKV infection. In human—but not mouse—cells, stimulator of IFN genes (STING)-dependent induction of IFN-β, -λ, and IFN-stimulated genes (ISGs) via cGAMP is suppressed by ZIKV, indicating the functional relevance of the cGMP-AMP synthase (cGAS)/STING-pathway in restricting ZIKV infection in rodents. Our data show that human, but not mouse, STING is indeed the target of proteases encoded by a broad panel of flaviviruses, including DENV, WNV, Japanese encephalitis virus (JEV), and ZIKV, but not YFV. Using a combined biochemical and genetic approach, we mapped residues critical for ZIKV NS2B3-mediated cleavage to R78 and G79 in the cytoplasmic loop of human STING (hSTING). These residues, which are only partially conserved in the murine ortholog of STING, appear important also for cleavage by DENV, JEV, and WNV NS2B3. Furthermore, we demonstrate that disruption of STING expression significantly increases the susceptibility of mouse cells to ZIKV in vitro. This enhanced permissivity is maintained during genetic complementation with human, but not murine, STING. STING-deficient mice, however, were not more permissive to ZIKV, suggesting that other redundant antiviral pathways efficiently control ZIKV infection in vivo. Collectively, our data demonstrate that STING is a direct target of the NS2B3 protease of ZIKV and several other flaviviruses, and that this viral-evasion mechanism is important in shaping the host tropism of ZIKV.

Results

ZIKV Infection Is Attenuated in Mouse but Not Primate Cells. To gain insights into the host range of ZIKV, we systematically tested the susceptibility and permissivity of dermal fibroblasts (DFs), which can readily be obtained, from a broad range of species. For our analysis, we limited ourselves to not only human and mouse cells but also select NHPs, including great apes (*Pan troglodytes*, *Pan paniscus*, *Gorilla gorilla*, *Pongo pygmaeus*), Old World monkeys (*Papio anubis*, *Macaca nemestrina*, *Macaca mulatta*), and one New World monkey (*Saimiri sciureus*) (Fig. 1*A*). All fibroblasts were infected with ZIKV (MR766) at a multiplicity of infection (MOI) of 1, the inoculum removed, cells washed 8 h following infection, and infectious viral particle release quantified daily by plaque-forming assays until 72 h postinfection (*SI Appendix*, Fig. S1). Although the viral titers of supernatants from all of the NHP and human DFs were largely similar, supernatant collected from mouse cells contained ∼50- to 100-fold less infectious virus 72 h postinfection (Fig. 1*B*). These data are consistent with previous observations demonstrating that immunocompetent mice are resistant to ZIKV and only support infection when antiviral pathways are blunted. Our results further suggest that ZIKV can efficiently evade such innate defenses in cells derived from evolutionarily diverse species, spanning from humans to great apes to New and Old World monkeys.

ZIKV Suppresses STING-Dependent Induction of Innate Immune Responses in Human but Not Mouse Cells. A variety of cell-intrinsic defense systems that antagonize viral infections exist in mammalian cells. Toll-like receptors (TLRs) and RIG-I–like receptors (RLRs; RIG-I and MDA5) are pattern-recognition receptors that sense viral RNA and engage the adaptor protein TRIF or MAVS (26) [also known as IPS-1 (27), VISA (28), and CARDIF (29)] to establish an antiviral state by the induction of type I IFNs and ISGs. Similarly, cGAS and STING (30), also known as transmembrane protein 173 (TMEM173), MITA (31), MPYS (32), and ERIS (33), have been identified as pattern-recognition receptors that promote

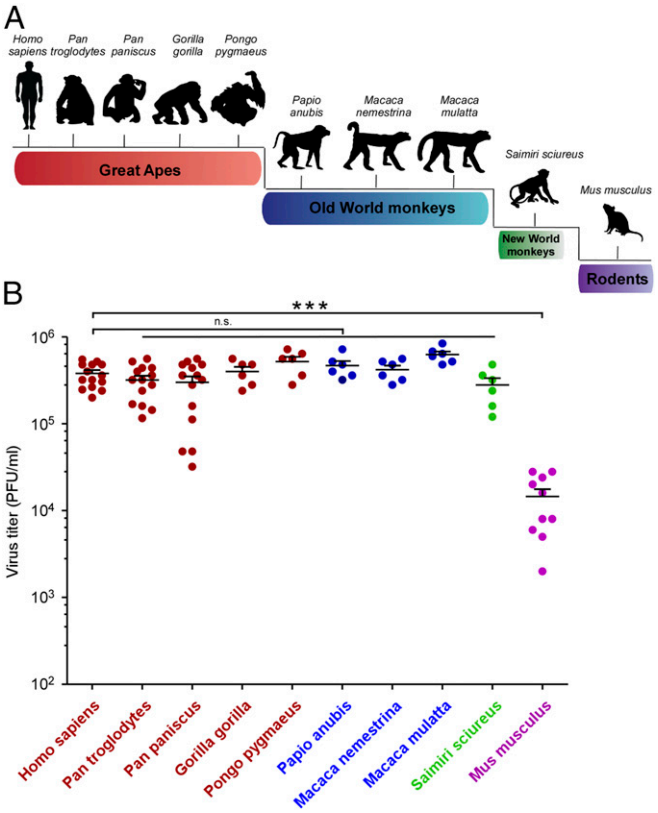

Fig. 1. DFs from different species have differing permissivity to ZIKV infection. (*A*) Schematic representation of the phylogenetic relationship of species included in this study. (*B*) Susceptibility of DFs from evolutionarily diverse species to ZIKV (MR766). Cells were washed twice with PBS 8 h postinfection. Cell medium was collected 3 d postinfection to determine viral titer. Error bars represent SDs of three experiments performed in duplicates and pooled: $n = 14$ for *Homo sapiens*, *P. troglodytes*, and *P. paniscus*; $n = 6$ for other species; n.s., nonsignificant; $P > 0.05$; ***$P < 0.001$ by one-way ANOVA with Tukey's HSD test.

IFN production in response to a range of DNA and RNA viruses (reviewed in ref. 34).

To directly test whether ZIKV infection compromises the ability of cells to mount antiviral responses via these pathways, we stimulated human or mouse fibroblasts with cGAMP or poly-inosinic:polyctidylic acid [poly(I:C)] 4 d postinfection with ZIKV (Fig. 2 and *SI Appendix*, Fig. S2*D*). Poly(I:C) is a synthetic double-stranded RNA analog primarily sensed by RLRs and TLR3, while cGAMP is the product of cGAS and triggers STING-dependent expression of IFN and ISGs. cGAMP robustly induced transcription of type I (IFN-β, approximately 300-fold, all compared with uninfected cells in the absence of stimulation) and type III (IFN-λ, approximately 20-fold) IFNs as well as MxA (approximately 30-fold) in naive mouse and human fibroblasts. In contrast, in human cells infected with ZIKV (strain MR766), IFN and ISG induction was markedly lower upon cGAMP stimulation compared to noninfected, cGAMP-stimulated cells: IFN-β was 6- to 20-fold lower (Fig. 2*A*), IFN-λ was 30- to 60-fold lower (Fig. 2*B*), and MxA 5- to 10-fold lower (Fig. 2*C*). Notably, we did not observe significant changes in expression of type I or type III IFN or MxA following stimulation with poly(I:C), suggesting that the RLR/TLR3 signaling axis by and large remains functionally intact during ZIKV infection. Furthermore, induction of IFN-β, -λ, and MxA was largely equivalent in mouse fibroblasts stimulated with cGAMP or poly(I:C) regardless of infection status (Fig. 2 *D*–*F*). This evident discrepancy in IFN and ISG induction by cGAMP

MICROBIOLOGY

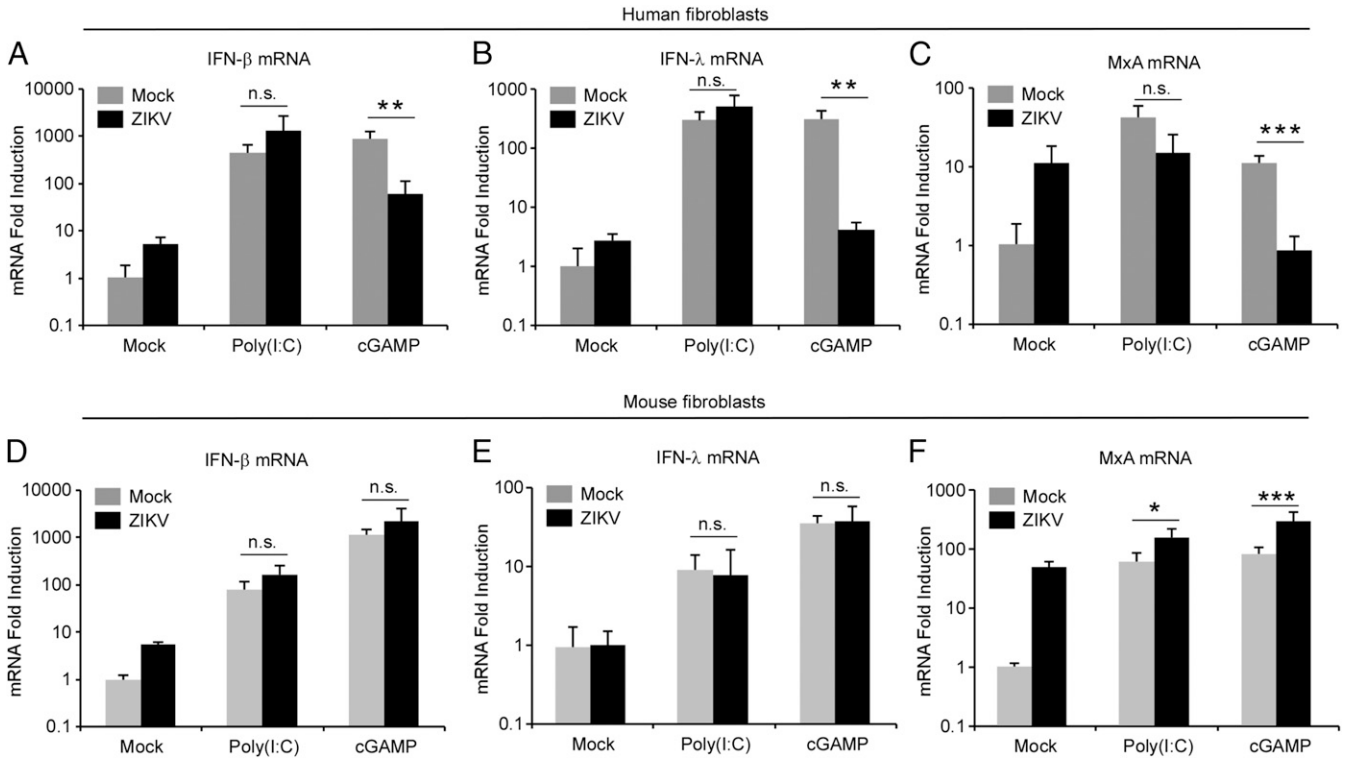

Fig. 2. ZIKV infection blocks cGAMP-induced IFN production in human DFs. (*A–C*) Human DFs were either mock-infected or infected with ZIKV (MR766) at an MOI of 1. Four days after infection, cells were transfected with poly(I:C) or stimulated with cGAMP. After stimulation, the cells were collected and total RNA were purified for qRT-PCR to determine expression of IFN-β (*A*), IFN-λ (*B*), and MxA (*C*). (*D–F*) ZIKV-infected or mock-infected mouse dermal fibroblasts were stimulated with poly(I:C) or cGAMP. qRT-PCR was performed to determine IFN-β (*D*), IFN-λ (*E*), and MxA (*F*) expression. Error bars represent SDs of three experiments performed in triplicate and pooled ($n = 9$): n.s., nonsignificant, $P > 0.05$; $^{*}P \leq 0.05$; $^{**}P < 0.01$; $^{***}P < 0.001$ by two-tailed Student's *t* test.

between ZIKV-infected human and mouse fibroblasts cannot simply be explained by the putative inability of ZIKV to infect mouse fibroblasts, as the frequency of ZIKV E-expressing cells was only fourfold different between human and mouse fibroblasts (*SI Appendix*, Fig. S2*D*). Collectively, these data strongly suggest that ZIKV selectively targets the cGAS/STING pathway to blunt cell-intrinsic antiviral defenses. To ascertain whether the impairment of the cGAS/STING pathway by ZIKV was strain-dependent, we validated our results with a second ZIKV isolate (Dakar 41671). Dakar 41671 similarly compromised the ability of human, but not mouse, fibroblasts to respond to cGAMP stimulation (*SI Appendix*, Fig. S2). Thus, this viral evasion mechanism appears to operate much more efficiently in human versus mouse cells, providing a potential explanation for the apparent differences in these species' susceptibility to infection.

STING Is the Target of Virally Encoded Proteases of Multiple Flaviviruses. STING acts downstream of cGAS and cGAMP and although the pathway is thought to be primarily involved in sensing bacterial and viral DNA, it has become increasingly evident that STING also plays an important role in restricting RNA virus infection in vitro and in vivo (35). Additionally, STING is antagonized by several (+) single-stranded RNA viruses, such as hepatitis C virus (HCV) (36, 37) and DENV (38–40). In the latter case, the DENV NS2B protein targets cGAS for degradation and thereby prevents mitochondrial DNA sensing during infection (41), suggesting that STING is an important restriction factor. To directly test whether STING is indeed a target of the ZIKV-encoded protease, we coexpressed a FLAG-tagged ZIKV NS2B3 along with HA-tagged human or mouse STING (mSTING) (Fig. 3*A*). Although ZIKV NS2B3 was capable of cleaving hSTING, we did not detect the characteristic cleavage product for mSTING. This differential proteolytic activity was not due to differences in the expression level of the viral protease as NS2B3 and its autoprocessed form NS3 were readily detectable (Fig. 3*A*, *Top*). Expectedly, coexpressing a catalytically inactive form of ZIKV NS2B3 did not result in proteolytic cleavage of either hSTING or mSTING. Of note, a hSTING mutant, in which residues 93–96 covering the previously proposed cleavage site for DENV NS2B3 (38, 40) were replaced with those of the mouse sequence (IHCM mutant), remained cleavable. To investigate more broadly this species-specific cleavage of STING by proteases of other flaviviruses closely related to ZIKV, we tested NS2B3 of DENV, JEV, WNV, and YFV. In accordance with previously published data, catalytically active DENV NS2B3 cleaved hSTING (38, 40) but did not seem to affect mSTING (Fig. 3 *B* and *C*). JEV and WNV NS2B3 followed a similar pattern, whereas the proteases of the YFV vaccine strain (YFV-17D) and virulent YFV (YFV-Asibi) were incapable of cleaving either hSTING or mSTING (Fig. 3 *B* and *D*). To demonstrate that endogenous STING is also subject to cleavage during infection, we infected human fibroblasts with MR766 and subjected cell lysates collected on day 3 postinfection to Western blot (Fig. 3*E*). Indeed, the characteristic cleavage product was readily detectable in infected but not in noninfected cells. Taken together, these data demonstrate that the NS2B3 protease of not only DENV—as previously reported (38–40)—but also ZIKV, JEV, and WNV can cleave hSTING but not mSTING, providing further evidence for the functional relevance of this pathway in shaping the host tropism of ZIKV and potentially other flaviviruses.

Mapping the ZIKV NS2B3 Protease Cleavage Site Within STING. Next, we aimed to determine the exact position where ZIKV NS2B3-mediated STING cleavage may occur. It was previously suggested that hSTING is cleaved by DENV between Arg-95 and Gly-96 (38,

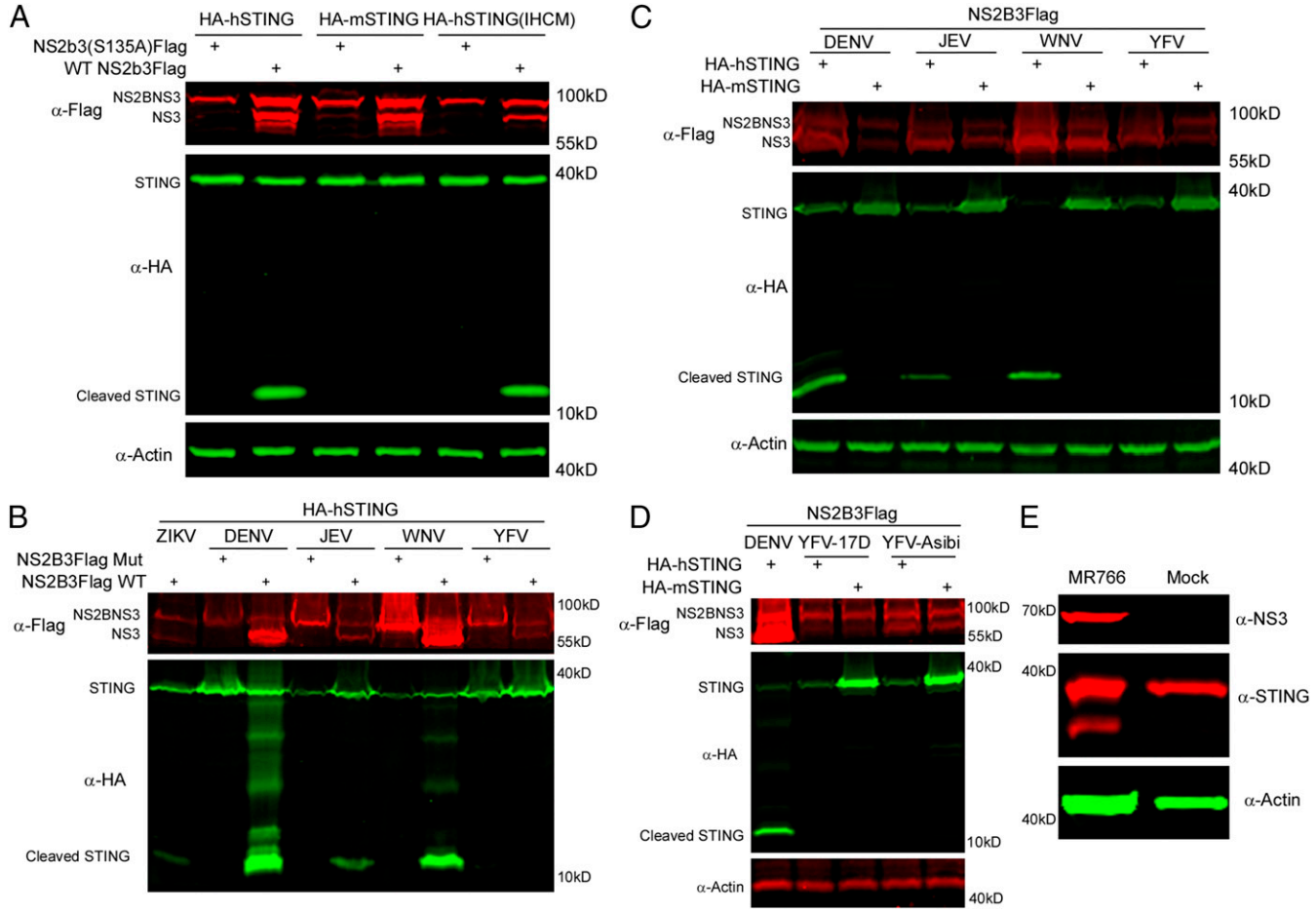

Fig. 3. Flavivirus protease-mediated cleavage of hSTING is a conserved mechanism to evade innate immunity. (*A*) HEK293T cells were cotransfected with hSTING, mSTING, or a human/mouse STING chimera in addition to Flag-tagged ZIKV NS2B3 or a proteolytically inactive mutant NS2B3(S135A). Lysates from transfected cells were prepared for immunoblotting with antibodies, as indicated. (*B*) Western blot of HEK293T cells transfected with hSTING and Flag-tagged NS2B3 or the protease NS2B3 mutant from the indicated flaviviruses. (*C*) Western blot of HEK293T cells transfected with human or mouse STING as indicated and the Flag-tagged NS2B3 from different flaviviruses. (*D*) Western blot of HEK293T cells transfected with the constructs expressing human or mouse STING as well as the Flag-tagged DENV, YFV-17D, or YFV-Asibi NS2B3 proteases. (*E*) Human DFs were infected with ZIKV (MR766) at an MOI of 2. Three days following infection, infected or noninfected (mock) cells were lysed in RIPA buffer supplemented with protease inhibitors. The cell lysate was analyzed by an immunobloting assay to detect ZIKV NS3, STING, and β-actin. Each experiment was repeated at least three times.

40) (Fig. 4*A*) within the third transmembrane domain (*SI Appendix*, Fig. S4). We aligned the amino acid sequences of STING across human, bonobo, chimpanzee, gorilla, orangutan, rhesus and pig-tailed macaques, olive baboon, squirrel monkey, and mouse, the same species whose fibroblasts we interrogated for susceptibility to ZIKV (Fig. 1). Although the overall protein sequences are largely conserved across all species (67.3–100% identity and 80.4–100% similarity compared with hSTING) (*SI Appendix*, Fig. S3), there were differences in the RG motif at position 95/96. The hSTING IHCM mutant, in which aa 93–96 of hSTING (LRRG) are replaced with the corresponding mouse sequence (IHCM), remained sensitive to ZIKV NS2B3 protease cleavage, indicating that the RG motif in positions 95/96 is not the cleavage site (Fig. 3*A*). We also noted another RG in positions 78/79 of the human sequence within the cytoplasmic loop of hSTING (Fig. 4*A* and *SI Appendix*, Fig. S4) and hypothesized that this may constitute another putative cleavage site. The protein sequences of the primate and rodent species we included here differ at positions 78 and 79, and thus conceivably are resistant to cleavage. To test whether STING from diverse primate species can be cleaved by the ZIKV protease, we coexpressed full-length STING sequences of representatives of great apes, New World and Old World monkeys, along with ZIKV NS2B3. In contrast to hSTING, neither chimpanzee, rhesus, nor squirrel monkey STING were cleaved (Fig. 4*B*). To specifically test the functional relevance of these positions in the cleavage of hSTING, we constructed point mutants, swapping the R78 with either a Q, which is present in the mouse and squirrel monkey sequences, or a W, which is present in bonobo and chimpanzee. Similarly, we replaced G79 with an aspartic acid as found in the Old World monkey species tested (olive baboon, pig-tailed and rhesus macaque). Notably, mutating the native R78/G79 to any of these three residues completely abrogated ZIKV NS2B3 cleavage (Fig. 4*C*). The cleavage by ZIKV NS2B3 likely occurs between positions 78 and 79, as the cleavage fragment is identical in size to the hSTING 1–78 truncation mutant but smaller than a form of STING truncated after residue 95 (Fig. 4*D*). Analysis of SNP data from the 1000 Genome Project revealed that four major nonsynonymous variants of hSTING are found in high frequencies [R232H, R293Q, G230A-R293Q (AQ) and R71H-G230A-R293Q (HAQ)] (42). Considering that R71 SNP is in close proximity to the ZIKV NS2B3 putative cleavage site in STING, we tested ZIKV NS2B3-mediated cleavage of the R71 isoform of STING. Our data suggest that the R71 SNP of STING does not interfere with the ZIKV NS2B3-mediated cleavage of STING (Fig. 4*D*).

We then assessed whether replacing the mouse, chimpanzee, or rhesus macaque STING residues at and around the presumed

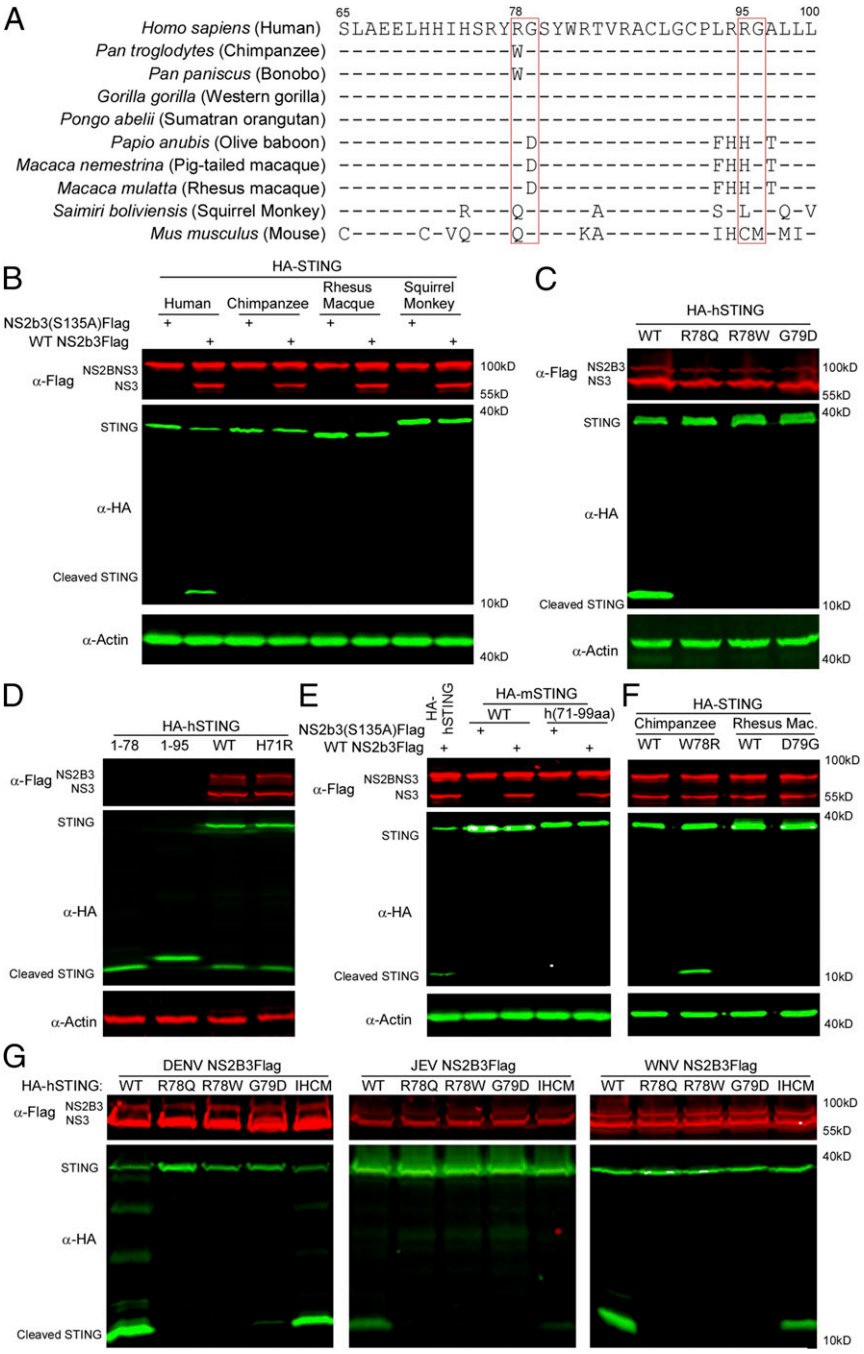

Fig. 4. Flavivirus proteases cleave hSTING at Arg-78. (*A*) Alignment of amino acids 68–100 of STING from different species. The putative cleavage sites $R^{78}G^{79}$ and $R^{95}G^{96}$ are indicated in the red boxes. (*B*) HEK293T cells were transfected with HA-tagged STING as indicated species and Flag-tagged ZIKV NS2B3(WT or S135A). Lysates of transfected cells were analyzed by immunoblotting with the antibodies indicated on the left. (*C* and *D*) HEK293T cells were transfected with the wild-type, truncated, or mutant constructs of hSTING as indicated and Flag-tagged ZIKV NS2B3. Lysates of transfected cells were prepared for immunoblotting with the antibodies indicated on the left. (*E* and *F*) Western blot of HEK293T cells transfected with the WT or humanized (amino acids 71–99 were replaced with the corresponding sequence of hSTING) mSTING, WT or humanized chimpanzee STING, WT or humanized rhesus macaque STING, as indicated, and Flag-tagged ZIKV NS2B3. (*G*) Western blots of HEK293T cells cotransfected with NS2B3 proteases from different flaviviruses (DENV, JEV, and WNV) plus the indicated constructs of hSTING or mutants. Each experiment was repeated at least three times and same results were obtained.

cleavage site with their human counterparts would facilitate cleavage by ZIKV NS2B3. While coexpression of mSTING[h71-99] or rhesus macaque STING[D79G] along with ZIKV NS2B3 did not yield the characteristic cleavage pattern (Fig. 4*E*), mutating the chimpanzee STING at residue W78 to the arginine present in the human protein at this position made the resultant chimpanzee STING[W78R] susceptible to ZIKV NS2B3 cleavage. This suggests that cleavage presumably depends on a specific conformation of full-length hSTING or other *cis*-acting elements that are preserved in chimpanzee STING, but not in our minimally humanized mSTING and rhesus macaque STING.

Of note, the NS2B3 proteases of DENV, JEV, and WNV appear to also cleave hSTING at the RG 78/79 position, as R78Q/W and G79D mutants were not cleavable (Fig. 4*G*). In

contrast, the hSTING IHCM mutant remained subject to proteolytic breakdown by DENV and WNV but not JEV NS2B3 (Fig. 4*G*). The results for the former stand in contrast to previously published data suggesting that the hSTING IHCM mutant is not cleaved by DENV NS2B3 (38) but are consistent with a very recent study demonstrating that hSTING is indeed cleaved between RG 78/79 by DENV NS2B3 (39).

Disruption of STING-Dependent Innate Immune Defenses Increases Permissiveness of Mouse Cells to ZIKV. Our data presented up to this point strongly suggest that the differential susceptibility of human and mouse cells to ZIKV appears to correlate with the ability of ZIKV NS2B3 to cleave hSTING but not mSTING. To directly test the impact of STING-dependent signaling on restricting ZIKV host tropism in murine cells, we performed loss-of-function and genetic complementation experiments (Fig. 5). We designed single-guide RNAs (sgRNAs) targeting human and mouse STING (two different sgRNAs for each species) and inactivated these genes in immortalized DFs from the respective species using CRISPR/Cas9. We generated two cell lines from each species lacking expression of endogenous human or mouse STING (Fig. 5*A*) and tested their permissiveness to ZIKV (MR766) infection. Although knocking out STING in human fibroblasts did not further augment permissivity to ZIKV (Fig. 5*B*), supernatants from infected mSTING knockout (KO) cells contained ~10–50 times more infectious virus throughout the 4-d time course (Fig. 5*C*). This higher permissivity was also reflected by the greater copy numbers of ZIKV RNA in the mSTING KO versus mSTING sufficient cells, while the levels of viral RNA remained similar in the hSTING KO and sufficient cells (Fig. 5*D*). The increased permissivity of the mouse cells is directly attributable to the lack of endogenous STING, as genetic complementation with mSTING reduced viral titers to those of sgRNA/GFP control cells (Fig. 5 *E* and *F*). Notably, expression of hSTING in mSTING KO fibroblasts subsequently infected with ZIKV recapitulated the phenotype observed in human cells. Intriguingly, the hSTING (R78Q), which is resistant to ZIKV NS2B3 cleavage, reduces ZIKV infection to a certain degree compared with WT hSTING. However, it does not completely recapitulate the mSTING phenotype to fully compromise ZIKV infection. This result suggests that ZIKV blocks hSTING antiviral function not only by NS2B3 protease-dependent hSTING cleavage, but conceivably also by an NS2B3 protease cleavage-independent mechanism.

Collectively, these data demonstrate that STING-dependent signaling is an important contributor to modulating the host range of ZIKV. Future studies are aimed at exploring the importance of cGAS/STING-mediated defenses to restrict ZIKV and, more generally, other flaviviruses in vivo.

STING-Deficient Mice Are Not Susceptible to ZIKV Infection. Next, we aimed to determine the impact of STING deficiency in vivo. To this end, we used the so-called golden ticket mouse (43), which harbors a missense mutation in exon 6 of the Sting gene

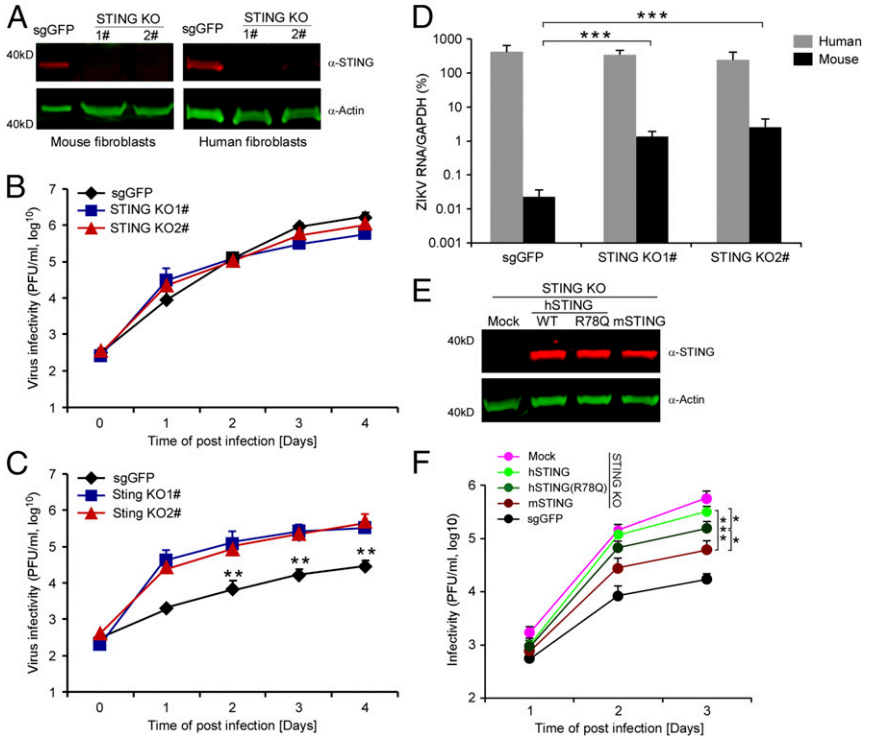

Fig. 5. STING restricts ZIKV infection in a species-dependent manner. (*A*) STING was knocked out from mouse or human fibroblasts with CRISPR/Cas9, as described in *Experimental Procedures*. KO efficiency was determined by Western blot analysis using antibodies against STING and β-actin, as indicated. (*B* and *C*) The cells were infected with ZIKV and the infectious kinetics were determined in the different cells. ZIKV titers were determined longitudinally by plaque assay of the supernatants from infected human (*B*) or mouse (*C*) fibroblasts sufficient or deficient for STING. Error bars represent the SD of the mean from one representative experiment three biological replicate samples and each experiment was repeated three times. $^{**}P < 0.01$ by one-way ANOVA. (*D*) Quantification of ZIKV RNA in infected human or mouse DFs (WT or STING KO) 5 d postinfection. Error bars represent the SD of the mean from one representative experiment three biological replicate samples and each experiment was repeated three times. $^{***}P < 0.001$ by one-way ANOVA. (*E* and *F*) Genetic complementation of mSTING KO DF with hSTING (WT or R78Q) or mSTING. After 5 d of lentivirus infection, hSTING (WT or R78Q) or mSTING expression was confirmed by Western blotting assay (*E*). Cells were subsequently infected with ZIKV (MR766) and infectious viral particle released were determined by plaque assay on Vero cells. Error bars represent SDs of $n = 4$ biological replicates: $^{*}P \leq 0.05$; $^{***}P < 0.001$ by one-way ANOVA. (*F*). This experiment was repeated two times.

(*Tmem173*^{Gt}), resulting in an isoleucine-to-asparagine change at amino acid 199 in the C terminus of the protein. Although STING-deficient mice have been previously infected with ZIKV, it was only reported that this strain does not succumb to infection (23), which does not necessarily mean that they are completely resistant to infection. We infected cohorts of *Tmem173*^{Gt} mice as well as WT control and IFN-αβ receptor-deficient (*Ifnar1*$^{-/-}$) mice, which are hypersusceptible to ZIKV infection (23). Consistent with previous reports, *Ifnar1*$^{-/-}$ mice lost significant weight and started to show signs of paralysis by day 6 postinfection, while WT control mice remained largely unaffected by viral challenge. Similarly, *Tmem173*^{Gt} mice did not develop clinically apparent symptoms and did not lose any weight over the study period (*SI Appendix*, Fig. S5). While *Ifnar1*$^{-/-}$ mice became highly viremic at day 2 postinfection and remained infected at day 6 postinfection, *Tmem173*^{Gt} mice—similar to the WT control animals—did not exhibit any elevated serum viremia levels over the same time frame (Fig. 6*A*). Consistently, ZIKV RNA was detected in the lungs, liver, spleen, kidneys, testes, brain, and spinal cord of *Ifnar1*$^{-/-}$ mice at the endpoint (day 6 postinfection) but remained at background levels in the two other groups of mice (Fig. 6*B*). Collectively, these data demonstrate that although STING-deficiency augments ZIKV replication in mouse cell lines, it is not sufficient in vivo and other redundant antiviral pathways that efficiently control ZIKV infection in vivo await identification.

Discussion

The host range of a given pathogen can be influenced by several parameters. A nonsusceptible or nonpermissive species may not possess the appropriate molecular factors or may have incompatible orthologs of factors needed for successful infection, such as receptors for a specific virus to enter host cells. Additionally, dominant restriction factors may actively interfere with one or more steps of a virus' life cycle (44). Alternatively, but not necessarily mutually exclusive, the varying abilities of a pathogen to evade and disrupt the immune response of a given host can also shape species tropism. There are numerous well-described examples of how differences in cell-intrinsic immunity impact the host tropism of human viral pathogens. For example, the capacity of hepatitis A virus to evade MAVS-mediated type I IFN responses defines its host-species range (45). Similarly, HCV replication is limited—in part—by STAT1-dependent IFN responses in murine hepatocytes in vitro (46) and in vivo (47). Several classic flaviviruses cannot readily overcome antiviral defenses in nonprimate cells. For example, both WNV and YFV-17D infection is attenuated by type I and III IFN signaling in mice (48, 49).

Similarly, ZIKV employs a variety of mechanisms to overcome antiviral immunity and ultimately establish infection in host cells. It was previously demonstrated that the ZIKV nonstructural proteins NS1, NS4B, and NS2B3 inhibit the induction of IFN and downstream ISGs through diverse strategies. NS1 and NS4B of ZIKV inhibit IFN-β signaling at the level of TANK-binding kinase 1 (50), while NS2B3 impairs the JAK-STAT signaling pathway by degrading Jak (51) and targeting STAT2 for degradation (52). Two recent studies showed that ZIKV—specifically several of its nonstructural proteins—inhibited induction of a luciferase reporter driven by the IFN-β promoter when stimulated with poly(I:C) or agonists of the RIG-I–like helicase pathway (50, 53). These observations would suggest that the RIG-I–MAVS–IKK pathway is inhibited by ZIKV, which is not fully supported by our data as we show that ZIKV-infected cells remain responsive to poly(I:C) stimulation, as evidenced by induction of endogenous IFN-β, -λ, and MxA mRNAs. However, it should be noted that the cell types [Huh7 hepatoma cells (53) and HEK293T cells (50) versus DFs in our study], specific ZIKV strains, and doses could impact the results. Furthermore, there is experimental evidence that by the cooperative actions of ZIKV NS1, NS4B, and NS2B3, viral infection is enhanced by blocking IFN-induced autophagic degradation of NS2B3 (51).

Here, we provide direct evidence that ZIKV also targets the cGAS/STING pathway by cleaving STING, impairing the cells' ability to induce ISGs in response to cGAMP, but not poly(I:C), stimulation. Proteolytic inactivation of STING appears to be a general mechanism shared by several other flaviviruses, including JEV, DENV (38–40, 54), and WNV, but not live-attenuated or virulent YFV. We found that the residues R78 and G79, located within the cytoplasmic loop of STING, are critical determinants for NS2B3-mediated cleavage. These observations stand in contrast to previously published observations for DENV NS2B3 that identified the STING cleavage site at position 95/96 within the third transmembrane domain (38, 40), but are consistent with more recently published data mapping the DENV protease cleavage site to positions 78/79 (39). While ZIKV NS2B3 can cleave STING after R95, the cleavage fragment has a higher molecular weight than that of the observed cleavage fragment, indicating that position 95/96 is unlikely the cleavage site in our experimental setting.

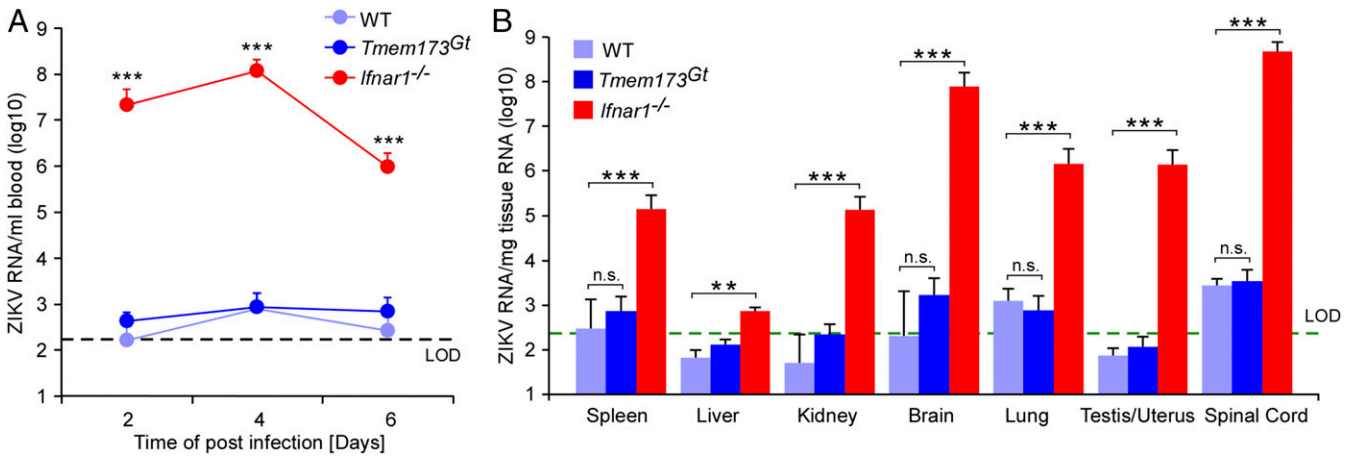

Fig. 6. STING-deficient mice are not susceptible to ZIKV infection. WT (C57BL/6), *Tmem173*^{Gt}, and *Ifnar1*$^{-/-}$ mice were infected with 10^3 plaque forming units of ZIKV virus (MR766) by an intravenous route. (*A*) ZIKV RNA in serum was quantified by qRT-PCR assay at indicated time point. Results are denoted as the ZIKV RNA genome equivalent per milliliter of blood. (*B*) At day 6 postinfection, the indicated tissues were harvested and ZIKV RNA levels analyzed by qRT-PCR. Results are denoted as the ZIKV RNA genome equivalent per microgram of total RNA from tissues. Error bars represent SDs of $n = 5$ mice per group. Statistical significance was determined using one-way ANOVA; n.s., nonsignificant; $P > 0.05$; $^{**}P < 0.01$; $^{***}P < 0.01$. LOD, limit of detection.

We did not detect cleavage by ZIKV, WNV, DENV, or JEV NS2B3 after exchanging the RG residues of human STING with those found at the same position (amino acids 78/79) in the STING orthologs of the species we tested. However, fibroblasts from all of the species examined, except for mice, were permissive to ZIKV infection. A potential explanation for this apparent discrepancy could be that ZIKV inactivates the cGAS/STING pathway in NHPs via a different mechanism, as has been shown for other flaviviruses. For example, prior studies found that DENV NS2B targets cGAS directly for degradation, preventing mitochondrial DNA sensing during infection (41). NS4B protein of other members of the *Flaviviridae* family—such as HCV, YFV, and DENV—can block STING function (36, 55). It is conceivable that ZIKV NS4B has a similar mechanism to further overcome human STING function. Alternatively, it is also conceivable that ZIKV can replicate in NHP cells, even in the presence of an intact cGAS/STING pathway, as other antiviral signaling pathways may already be blunted, thereby creating a host environment conducive to ZIKV replication.

Mechanistically deciphering how ZIKV evades cell-intrinsic immunity has aided in the development of experimental animal models used to study ZIKV pathogenesis and test antiviral therapies and vaccine candidates. Several studies have independently proven that *Ifnar1*$^{-/-}$ mice are hypersusceptible and succumb to ZIKV infection (8, 23, 24, 56). These findings are further corroborated by observations that STAT2$^{-/-}$ and IFN regulatory factor-3, -5, and -7 triple-knockout mice are highly susceptible to ZIKV infection, recapitulating virus spread to the central nervous system, gonads, and other visceral organs, and displaying neurological symptoms (23).

Although IFN-αβR–dependent responses clearly play a crucial role in restricting ZIKV in vivo, it remains less well understood what other antiviral signaling pathways antagonize ZIKV. In this study, we demonstrate that STING-dependent signaling is important for limiting ZIKV infection in mouse cells. These observations are consistent with previous findings that DENV NS2B protein targets cGAS for degradation and prevents mitochondrial DNA sensing during infection (41). We selected NHP species covering ∼35 My of evolution: great apes (*P. troglodytes*, *P. paniscus*, *G. gorilla*, *P. pygmaeus*), which are most closely related to humans; three Old World monkey species (*P. anubis*, *M. nemestrina*, *M. mulatta*), and one New World species (*S. sciureus*), which are commonly used in biomedical research. Additionally, for a more distant point in evolutionary time (approximately 65 My since divergence), we included mouse. To our knowledge, this is the most comprehensive analysis of ZIKV's ability to infect and replicate in cells, specifically DFs, from diverse species. Our study provides direct evidence that ZIKV establishes robust infections in fibroblasts isolated from humans, great apes, New and Old World monkeys, but is restricted in mouse cells. The fact that ZIKV can establish robust infections in the primate species but not in rodents suggests that in the latter, more distantly related species, STING-dependent activation of IFN-signaling has a more profound impact on overall antiviral defenses. Genetic disruption of STING in mouse fibroblasts significantly augmented ZIKV infection. These observations are corroborated by results from chemical high-throughput screens, which found that a dispiro diketopiperzine (DSDP) compound induced a cytokine response in a manner dependent on the expression of functional hSTING but not mSTING. Treatment with DSDP induced an IFN-dominated cytokine response in human skin fibroblasts and peripheral blood mononuclear cells, leading to potent suppression of YFV, DENV, and ZIKV replication (57). Of note, in contrast to IFN-αβR–deficient mice, MAVS, TRIF, or STING KO mice do not succumb to ZIKV infection (23, 58). However, death is a crude readout and not necessarily relevant as ZIKV infection in humans is usually not life-threatening. Our in vivo data show that genetic disruption of the cGAS/STING pathway does not result in higher ZIKV viremia in rodents. Presumably, other redundant cell-intrinsic antiviral defense and conceivably cellular and humoral immune responses act to efficiently control ZIKV infection in vivo. Nonetheless, these data suggest that ZIKV infection is restricted in murine hosts by more than one antiviral-sensing pathway that is ultimately dependent on the actions of IFNs.

Experimental Procedures

Additional procedures are described in detail in the *SI Appendix*. All mice were bred in the Laboratory Animal Resource Center of Princeton University. All animal experiments were performed in accordance to a protocol (number 1930) reviewed and approved by the Institution Animal Care and Use Committee of Princeton University.

Cell Culture. HEK293T (ATCC CRL-3216) and Vero cells (ATCC CCL-81) were obtained from the American Type Culture Collection (ATCC). Human or mouse immortalized fibroblasts were achieved by transduction of SV40 T antigen. HEK293T, human and mouse DFs and Vero cells were all cultured in DMEM (LifeTechnologies) containing 10% FBS, 100 U/mL penicillin, and 100 mg/mL streptomycin.

Viral Stocks and Viral Titration. The ZIKV strains (MR766, Dakar 41671) were kindly provided by Tom Shenk, Princeton University, Princeton, NJ and Michael Diamond, Washington University in St. Louis, St. Louis, MO, respectively. To produce viral stocks, Vero cells were seeded into T150 flasks (5 million cells per flask) and cultured for 24 h. The cells were infected with 10 mL of diluted virus (MOI = 0.01) for 2 h, after which another 5 mL of medium was added to the flask. Culture supernatants were harvested 5 d postinfection and filtered using 0.45-μm syringe filters. Viral stocks were aliquoted and stored at −80 °C.

To determine ZIKA virus titers, Vero cells were plated in 24-well plates 1 d before the titration assay. The Vero cells were infected with supernatants containing ZIKV in a 10-fold dilutions series for 2 h and inocula subsequently aspirated. Cells were overlaid with 2% methylcellulose (Sigma-Aldrich)/DMEM, grown for 4 d, and then fixed using 4% (wt/vol) paraformaldehyde. The cells were washed with PBS once and then stained with Crystal violet (0.1% Crystal violet in 20% ethanol) for 15 min. After staining, the wells were extensively washed with water and dried. The resulting plaques were counted, and the number of plaque forming units per milliliter was calculated.

Statistical Analysis. Student's *t* test or one-way ANOVA with Tukey's honestly significant difference (HSD) test was used to test for statistical significance of the differences between the different group parameters. *P* values of less than 0.05 were considered statistically significant.

ACKNOWLEDGMENTS. We thank Drs. Tom Shenk (Princeton University) and Michael Diamond (Washington University in St. Louis) for sharing the Zika virus strains of MR766 and Dakar41671, respectively; Dr. Sergei Kotenko (Rutgers University) for providing the *Ifnar*$^{-/-}$ mice; members of the A.P. laboratory for critical discussions and comments on the manuscript; and Christina DeCoste and Katherine Rittenbach and the Molecular Biology Flow Cytometry Resource Facility, which is partially supported by the Cancer Institute of New Jersey Cancer Center Support Grant P30CA072720. This work was supported by National Institutes of Health Grants R01 AI107301 and R21 AI117213 (to A.P.); and a grant from the Grand Health Challenge program from Princeton University and an Investigator in Pathogenesis Award by the Burroughs Wellcome Fund (to A.P.). Q.D. and L.W. are supported by New Jersey Commission on Cancer Research Postdoctoral Fellowships DHFS16PPC007 (to Q.D.) and DFHS17PPC011 (to L.W.).

1. Morens DM, Fauci AS (2013) Emerging infectious diseases: Threats to human health and global stability. *PLoS Pathog* 9:e1003467.
2. Bhatt S, et al. (2013) The global distribution and burden of dengue. *Nature* 496:504–507.
3. Dick GW (1953) Epidemiological notes on some viruses isolated in Uganda; yellow fever, Rift Valley fever, Bwamba fever, West Nile, Mengo, Semliki forest, Bunyamwera, Ntaya, Uganda S and Zika viruses. *Trans R Soc Trop Med Hyg* 47:13–48.
4. Baud D, Gubler DJ, Schaub B, Lanteri MC, Musso D (2017) An update on Zika virus infection. *Lancet* 390:2099–2109.
5. Liu Y, et al. (2017) Evolutionary enhancement of Zika virus infectivity in *Aedes aegypti* mosquitoes. *Nature* 545:482–486.
6. Li C, et al. (2016) Zika virus disrupts neural progenitor development and leads to microcephaly in mice. *Cell Stem Cell* 19:120–126.

7. Retallack H, et al. (2016) Zika virus cell tropism in the developing human brain and inhibition by azithromycin. *Proc Natl Acad Sci USA* 113:14408–14413.
8. Govero J, et al. (2016) Zika virus infection damages the testes in mice. *Nature* 540: 438–442.
9. Rausch K, et al. (2017) Screening bioactives reveals nanchangmycin as a broad spectrum antiviral active against Zika virus. *Cell Rep* 18:804–815.
10. Barrows NJ, et al. (2016) A screen of FDA-approved drugs for inhibitors of Zika virus infection. *Cell Host Microbe* 20:259–270.
11. Zmurko J, et al. (2016) The viral polymerase inhibitor 7-Deaza-2′-C-methyladenosine is a potent inhibitor of in vitro Zika virus replication and delays disease progression in a robust mouse infection model. *PLoS Negl Trop Dis* 10:e0004695.
12. Estoppey D, et al. (2017) The natural product cavinafungin selectively interferes with Zika and dengue virus replication by inhibition of the host signal peptidase. *Cell Rep* 19:451–460.
13. Hercík K, et al. (2017) Adenosine triphosphate analogs can efficiently inhibit the Zika virus RNA-dependent RNA polymerase. *Antiviral Res* 137:131–133.
14. Xu M, et al. (2016) Identification of small-molecule inhibitors of Zika virus infection and induced neural cell death via a drug repurposing screen. *Nat Med* 22:1101–1107.
15. Richner JM, et al. (2017) Modified mRNA vaccines protect against Zika virus infection. *Cell* 169:176.
16. Pardi N, et al. (2017) Zika virus protection by a single low-dose nucleoside-modified mRNA vaccination. *Nature* 543:248–251.
17. Dowd KA, et al. (2016) Rapid development of a DNA vaccine for Zika virus. *Science* 354:237–240.
18. Larocca RA, et al. (2016) Vaccine protection against Zika virus from Brazil. *Nature* 536: 474–478.
19. Abbink P, et al. (2016) Protective efficacy of multiple vaccine platforms against Zika virus challenge in rhesus monkeys. *Science* 353:1129–1132.
20. Dick GW, Kitchen SF, Haddow AJ (1952) Zika virus. I. Isolations and serological specificity. *Trans R Soc Trop Med Hyg* 46:509–520.
21. Newman C, Friedrich TC, O'Connor DH (2017) Macaque monkeys in Zika virus research: 1947-present. *Curr Opin Virol* 25:34–40.
22. Mestas J, Hughes CC (2004) Of mice and not men: Differences between mouse and human immunology. *J Immunol* 172:2731–2738.
23. Lazear HM, et al. (2016) A mouse model of Zika virus pathogenesis. *Cell Host Microbe* 19:720–730.
24. Aliota MT, et al. (2016) Characterization of lethal Zika virus infection in AG129 mice. *PLoS Negl Trop Dis* 10:e0004682.
25. Tripathi S, et al. (2017) A novel Zika virus mouse model reveals strain specific differences in virus pathogenesis and host inflammatory immune responses. *PLoS Pathog* 13:e1006258.
26. Seth RB, Sun L, Ea CK, Chen ZJ (2005) Identification and characterization of MAVS, a mitochondrial antiviral signaling protein that activates NF-kappaB and IRF 3. *Cell* 122: 669–682.
27. Kawai T, et al. (2005) IPS-1, an adaptor triggering RIG-I- and Mda5-mediated type I interferon induction. *Nat Immunol* 6:981–988.
28. Xu LG, et al. (2005) VISA is an adapter protein required for virus-triggered IFN-beta signaling. *Mol Cell* 19:727–740.
29. Meylan E, et al. (2005) Cardif is an adaptor protein in the RIG-I antiviral pathway and is targeted by hepatitis C virus. *Nature* 437:1167–1172.
30. Ishikawa H, Barber GN (2008) STING is an endoplasmic reticulum adaptor that facilitates innate immune signalling. *Nature* 455:674–678.
31. Zhong B, et al. (2008) The adaptor protein MITA links virus-sensing receptors to IRF3 transcription factor activation. *Immunity* 29:538–550.
32. Jin L, et al. (2008) MPYS, a novel membrane tetraspanner, is associated with major histocompatibility complex class II and mediates transduction of apoptotic signals. *Mol Cell Biol* 28:5014–5026.
33. Sun W, et al. (2009) ERIS, an endoplasmic reticulum IFN stimulator, activates innate immune signaling through dimerization. *Proc Natl Acad Sci USA* 106:8653–8658.
34. Crowl JT, Gray EE, Pestal K, Volkman HE, Stetson DB (2017) Intracellular nucleic acid detection in autoimmunity. *Annu Rev Immunol* 35:313–336.
35. Ma Z, Damania B (2016) The cGAS-STING defense pathway and its counteraction by viruses. *Cell Host Microbe* 19:150–158.
36. Ding Q, et al. (2013) Hepatitis C virus NS4B blocks the interaction of STING and TBK1 to evade host innate immunity. *J Hepatol* 59:52–58.
37. Nitta S, et al. (2013) Hepatitis C virus NS4B protein targets STING and abrogates RIG-I-mediated type I interferon-dependent innate immunity. *Hepatology* 57:46–58.
38. Aguirre S, et al. (2012) DENV inhibits type I IFN production in infected cells by cleaving human STING. *PLoS Pathog* 8:e1002934.
39. Stabell AC, et al. (2018) Dengue viruses cleave STING in humans but not in nonhuman primates, their presumed natural reservoir. *eLife* 7:e31919.
40. Yu CY, et al. (2012) Dengue virus targets the adaptor protein MITA to subvert host innate immunity. *PLoS Pathog* 8:e1002780.
41. Aguirre S, et al. (2017) Dengue virus NS2B protein targets cGAS for degradation and prevents mitochondrial DNA sensing during infection. *Nat Microbiol* 2:17037.
42. Abecasis GR, et al.; 1000 Genomes Project Consortium (2010) A map of human genome variation from population-scale sequencing. *Nature* 467:1061–1073, and erratum (2011) 473:544.
43. Sauer JD, et al. (2011) The N-ethyl-N-nitrosourea-induced Goldenticket mouse mutant reveals an essential function of Sting in the in vivo interferon response to *Listeria monocytogenes* and cyclic dinucleotides. *Infect Immun* 79:688–694.
44. Douam F, et al. (2015) Genetic dissection of the host tropism of human-tropic pathogens. *Annu Rev Genet* 49:21–45.
45. Hirai-Yuki A, et al. (2016) MAVS-dependent host species range and pathogenicity of human hepatitis A virus. *Science* 353:1541–1545.
46. Vogt A, et al. (2013) Recapitulation of the hepatitis C virus life-cycle in engineered murine cell lines. *Virology* 444:1–11.
47. Dorner M, et al. (2013) Completion of the entire hepatitis C virus life cycle in genetically humanized mice. *Nature* 501:237–241.
48. Lazear HM, et al. (2015) Interferon-λ restricts West Nile virus neuroinvasion by tightening the blood-brain barrier. *Sci Transl Med* 7:284ra59.
49. Douam F, et al. (2017) Type III interferon-mediated signaling is critical for controlling live attenuated yellow fever virus infection in vivo. *MBio* 8:e00819-17.
50. Xia H, et al. (2018) An evolutionary NS1 mutation enhances Zika virus evasion of host interferon induction. *Nat Commun* 9:414.
51. Wu Y, et al. (2017) Zika virus evades interferon-mediated antiviral response through the co-operation of multiple nonstructural proteins in vitro. *Cell Discov* 3:17006.
52. Grant A, et al. (2016) Zika virus targets human STAT2 to inhibit type I interferon signaling. *Cell Host Microbe* 19:882–890.
53. Van der Hoek KH, et al. (2017) Viperin is an important host restriction factor in control of Zika virus infection. *Sci Rep* 7:4475.
54. Liu H, et al. (2017) Endoplasmic reticulum protein SCAP inhibits dengue virus NS2B3 protease by suppressing its K27-linked polyubiquitylation. *J Virol* 91:e02234-16.
55. Ishikawa H, Ma Z, Barber GN (2009) STING regulates intracellular DNA-mediated, type I interferon-dependent innate immunity. *Nature* 461:788–792.
56. Dowall SD, et al. (2016) A susceptible mouse model for Zika virus infection. *PLoS Negl Trop Dis* 10:e0004658.
57. Liu B, et al. (2017) A cell-based high throughput screening assay for the discovery of cGAS-STING pathway agonists. *Antiviral Res* 147:37–46.
58. Piret J, Carbonneau J, Rhéaume C, Baz M, Boivin G (2018) Predominant role of IPS-1 over TRIF adaptor proteins in early innate immune response against Zika virus in mice. *J Gen Virol* 99:209–218.